On the strength of the carbon nanotube-based space elevator cable: from nanomechanics to megamechanics

Nicola M Pugno

Department of Structural Engineering, Politecnico di Torino, Corso Duca degli Abruzzi 24, 10129, Italy

E-mail: nicola.pugno@polito.it

Abstract

In this paper various deterministic and statistical models, based on new quantized theories proposed by the author, are presented for estimating the strength of a real, and thus defective, space elevator cable. The cable, ~100 000 km in length, is composed of carbon nanotubes, ~100 nm long: thus, its design involves nanomechanics and megamechanics. The predicted strengths are extensively compared with the experimental and atomistic simulation results for carbon nanotubes available in the literature. All these approaches unequivocally suggest that the megacable strength will be reduced by a factor at least of ~70% with respect to the theoretical nanotube strength, today (erroneously) assumed in the cable design. The reason is the unavoidable presence of defects in so huge a cable. Preliminary in-silicon tensile experiments confirm the same finding. The deduced strength reduction is sufficient to place in doubt the effective realization of the space elevator, that if built as designed today will certainly break (in the author's opinion). The mechanics of the cable is also revised and possible damage sources discussed.

(Some figures in this article are in colour only in the electronic version)

Invited paper presented at Nanoscience and Nanotechnology 2005

1. Introduction

A space elevator (figure 1) basically consists of a cable attached to the Earth's surface for carrying payloads into space (Artsutanov 1960). If the cable is long enough, i.e., around 150 000 km (reducible by a counterweight), the centrifugal forces exceed the gravity of the cable, that will work under tension (Pearson 1975). The elevator would stay fixed geosynchronously. Once sent far enough, climbers would be accelerated by the Earth's
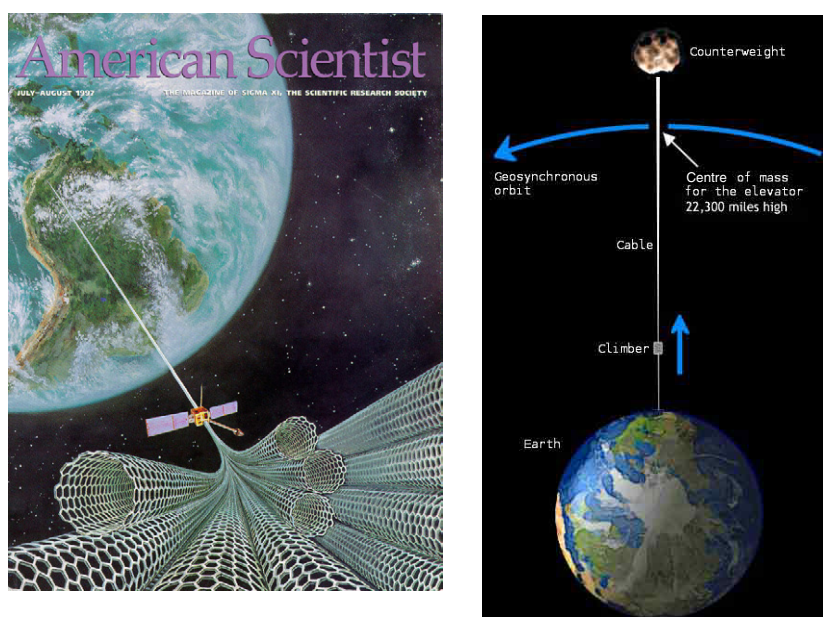
Figure 1. The cover of the American Scientist magazine (July–August 1997) reporting an artistic conception of the space elevator (left); and its structural scheme (right, downloaded from Wikipedia—the free encyclopaedia).

rotational energy. It is clear that a space elevator would revolutionize the methodology for carrying payloads into space, and in addition at 'low' cost. On the other hand, its design is very challenging.

The most critical component in the space elevator design is undoubtedly the cable, that requires a material with very high strength and low density. Considering a cable with constant section and a vanishing tension at the planet surface, the maximum stress, reached at the geosynchronous orbit (GEO), is for the Earth equal to 63 GPa, even if a low carbon density ($1300\,\mathrm{kg\,m^{-3}}$) is assumed for the cable. Only recently, since the discovery of carbon nanotubes (Iijima 1991), has such a large strength been experimentally observed (Yu *et al* 2000a, 2000b), during tensile tests of ropes composed of single-walled carbon nanotubes or multiwalled carbon nanotubes, expected to have an ideal strength of about 100 GPa. Note that for steel (density of $7900\,\mathrm{kg\,m^{-3}}$, assumed strength of 5 GPa) the maximum stress expected in the cable is 383 GPa, whereas for Kevlar (density of $1440\,\mathrm{kg\,m^{-3}}$, strength of 3.6 GPa) the maximum stress is 70 GPa, both much higher than their strengths. However, an optimized cable design must consider a uniform tensile stress profile (Pearson 1975) rather than a constant cross section area. Accordingly, the cable could be built of any material (Pearson 1975) by simply using a large enough 'taper ratio', i.e., the maximum cross section area (at GEO) over its minimum value (at the Earth's surface). For example, for steel this value is 10^{33}, for Kevlar it is 2.6×10^8 and for carbon nanotubes it is only 1.9. Since the mass of the cable depends on the taper ratio, the feasibility of the space elevator seems to become only plausible currently thanks to the discovery of carbon nanotubes (Edwards 2000, 2003). The cable would obviously represent the largest engineering structure, hierarchically designed from the nanoscale (single nanotube with length of the order of a hundred nanometres) to the megascale (space elevator cable with a length of the order of a hundred megametres).

Unfortunately, the presence of even a few vacancies in a single nanotube seems to play a dramatic role, as suggested by quantized fracture mechanics (QFM) criteria (Pugno 2002, 2004b, 2006b; Pugno and Ruoff 2004). And in such a huge cable we expect pre-existing defects not only for statistical reasons (Carpinteri and Pugno 2005) but also as a consequence of damage nucleation, e.g., due to micrometeorite or low Earth orbit object impacts and atomic oxygen erosion. After a review on the mechanics of the cable, the effect on the strength of the damage types mentioned is considered. Accordingly, different deterministic and statistical models are presented for estimating the strength of a real, thus defective, carbon nanotube-based space elevator cable. All these methods suggest expecting a megacable strength reduced by a factor of at least ~70% with respect to the theoretical nanotube strength, corresponding to a mass increment larger than 300%. Thus, the deduced strength reduction is sufficient to place in doubt the effective feasibility of the space elevator that, as designed today and according to the author's analysis and opinion, will undoubtedly break. Experiments and atomistic simulations, based on molecular or quantum mechanics, for carbon nanotubes confirm our argument. Size effects deduced by in-silicon experiments for carbon nanotube-based ropes confirm the strength reduction mentioned, in agreement with the first observations on the strength of metre-long nanotube-based ropes (Zhang *et al* 2005).

Thus, the general optimism as regards the effective realization of the space elevator (in 15 years for $ 10B; see Edwards (2000, 2003); Edwards and Westling (2003)) is placed in doubt by the role of defects in the cable: as we have not been able to build a large glass cable possessing the strength of a glass whisker, perhaps we will face a similar limit during the practical realization of the space elevator cable, and certainly if the design of the cable is not dramatically reconsidered. Accordingly, a detailed analysis on the role of defects in the cable seems to be crucial: formally, in addition to strength and density, the fracture toughness has to be taken into account and cannot be further neglected. The QFM criteria introduced by the author could help in solving, if a solution exists, the problem of a correct nanostructured megacable design, whereas classical atomistic simulations or experimental analyses remain unrealizable due to the tremendous size of the megacable.

2. From nanomechanics to megamechanics

As mentioned, experiments and atomistic simulations cannot be performed on so huge a cable. Thus, we need a theory able to treat objects spanning from the nanoscale to the megascale. We demonstrate here that this theory must include a characteristic length, governing the size scale considered, in contrast to the classical theories of elasticity and in particular linear elastic fracture mechanics (LEFM; Griffith 1921). Furthermore, LEFM has recently been generalized, relaxing the hypothesis of a continuum crack propagation (Pugno 2004a, 2004b, 2006a, 2006b; Pugno and Ruoff 2004), introducing in a natural way a characteristic length, i.e., the 'fracture quantum'. In this section we apply such a treatment to the smallest and to the largest object that in our planet fall down in the domain of mechanics, i.e., a nanotube, having a radius of a few nanometres, and the Earth itself, which has a radius of a few megametres. Note that these two objects are connected in the space elevator. We are going to show that a quantized theory successfully explains the deviations observed in the classical continuous counterparts, through the introduction of a fracture quantum, that varies from a fraction of a nanometre to several kilometres.

Let us consider the well-known Neuber (1958) and Novozhilov (1969) approach, that is the stress analogue of the energy-based QFM. It implies considering instead of the local stress, the corresponding force acting on a fracture quantum of length a, or equivalently the mean value of the stress σ along it. By applying this theory for predicting the failure stress σ_f of

a nanotube with a nanohole of radius R around which a stress field σ arises, i.e. by setting $\langle\sigma\rangle_a = \sigma_{th}$ where σ_{th} is the theoretical material strength, we deduce the following failure stress σ_f (Pugno and Ruoff 2004):

$$\frac{\sigma_f}{\sigma_{th}} = \frac{2x^3 + 6x^2 + 6x + 2}{6x^3 + 11x^2 + 8x + 2}, \qquad x = R/a. \tag{1}$$

Note that according to the elasticity and by imposing the maximum stress equal to the material strength, i.e., $\sigma_{max} = \sigma_{th}$, the prediction would be simply $\sigma_f/\sigma_{th} = 1/3$. In contrast, equation (1) implies $\sigma_f/\sigma_{th} = 1/3$ only for $x \to \infty$ (large holes; equation (1) does not consider boundary interactions), whereas for $x \to 0$, $\sigma_f/\sigma_{th} = 1$, i.e., holes with vanishing size do not affect the structural strength. A similar result is obtained by applying QFM, i.e., $\sqrt{\langle K^2\rangle_a} = K_C$, where K is the stress intensity factor (here at the tip of a mode I crack, emanating from the hole) and K_C is the fracture toughness of the material: in particular we found $\sigma_f/\sigma_{th}(x \to \infty) = 1/3.36$ and $\sigma_f/\sigma_{th}(x \to 0) = 1$. QFM is based on the energy balance for a quantized crack growth; thus basically it is derived from the classical Griffith's energy balance replacing the differentials by the finite differences. Mielke *et al* (2004) and Zhang *et al* (2005) performed quantum mechanical calculations using density functional theory and semiempirical methods and molecular mechanics to explore the role of vacancy defects in the fracture of carbon nanotubes under tension. Equation (1) closely describes their predictions on strength of nanotubes containing pinhole defects, as we will discuss in detail in section 5. An example of a comparison is given by the dashed line (equation (1)) and the rhombs (atomistic simulations on a [29, 29] carbon nanotube) reported in figure 2(a). Instead of using the fracture quantum a as a best fit parameter, we have more physically considered $a \approx 2.5$ Å, that is the distance between two adjacent chemical bonds broken during fracture (figure 2(b)): thus, the agreement is remarkable, as the deviation from the classical value of $1/3$.

On the other hand, let us consider the coefficient of geostatic stress, i.e., the ratio between the horizontal and vertical geostatic stresses (a fundamental parameter for tunnelling design). The vertical stress at a depth z is given by $\sigma_V = \gamma z$, where γ is the specific weight of the Earth's crust. Thus, the horizontal stress is given according to elasticity by $\sigma_H = v/(1 - v)\sigma_V$, where v is Poisson's ratio, and consequently the coefficient of geodetic stress becomes $K_0 = v/(1 - v)$ (~ 0.4). In contrast, after a huge experimental analysis Brown and Hoek (1978) found the coefficient of geodetic stress in the form $K \approx K_0 + C/z$ in which $C \approx 1$ km represents a corrective term, not expected from classical elasticity. Simply by considering instead of σ_H its quantized version, i.e., $\sigma_H^* = \frac{1}{a}\int_z^{z+a} \sigma_H \, dz$, as a method for including the effect of the layered crust structure of the Earth, we deduce

$$K = \frac{\sigma_H^*}{\sigma_V} = K_0 + \frac{K_0 a}{2z}, \tag{2}$$

i.e., exactly the experimental relation, with $C = K_0 a/2$. Thus, in this context, $a \approx 5$ km.

Accordingly, at the nanoscale a is found to be of the order of the ångström, whereas at the megascale it is of the kilometre order. Thus, continuum theories, simply assuming $a = 0$, are not appropriate in our multiscale context. This example shows that in general a simple but useful quantized elasticity can be formulated by replacing the stress σ with its mean value around a volume quantum a^3, i.e., $\sigma \to \langle\sigma\rangle_{a^3}$, recovering classical (local) elasticity only in the limited case of $a \to 0$, and extending the Neuber's (1958) and Novozhilov's (1969) approach also for problems that do not involve a crack propagation.

Similarly we expect a very large fracture quantum in the study of geophysics, e.g., treating earthquakes as fracture instabilities in faults. In addition, the dynamic version of QFM (Pugno 2004b, 2006b) suggests the existence of an (incubation) time quantum for crack propagation, related to the time needed to generate a fracture quantum: such a time delay has been observed,
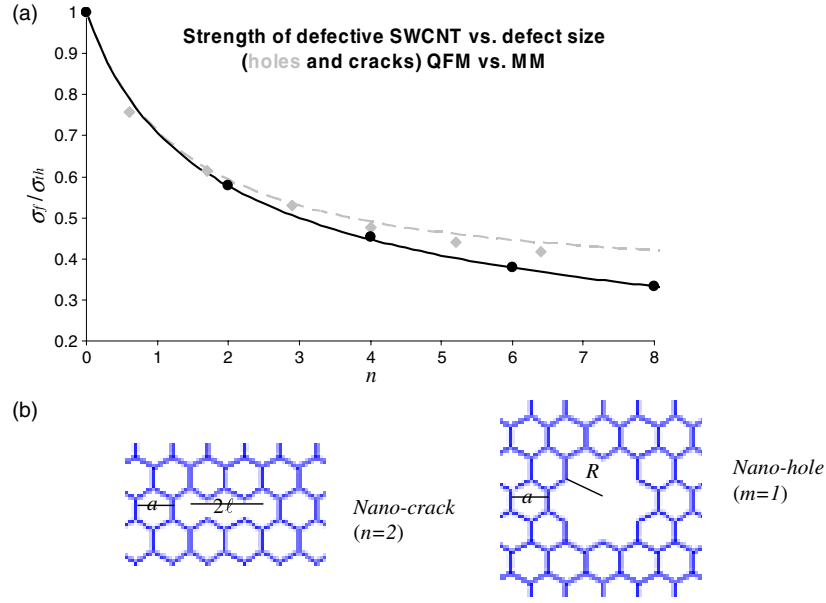
Figure 2. (a) Strength of defective SWCNT versus hole size defined as $n = 2R/a$ (QFM, dashed line; rhombs, atomistic simulations), or versus crack length $n = 2l/a$ (QFM, continuous line; points, atomistic simulations); the fracture quantum $a \approx 2.5$ Å is fixed identical to the distance between adjacent broken chemical bonds, thus not as a best fit parameter. (b) Defect and fracture quantum sizes: $n = 2$ denotes a nanocrack formed on removing two adjacent chemical bonds, $m = 1$ denotes a nanohole formed on removing the first carbon atom perimeter (six atoms); the applied tensile load is vertical.

of the order of microseconds, in impact failures of small specimens (see Pugno 2004b, 2006b), but of several hours during earthquake triggering (Gombers and Johnson 2005), confirming our argument.

This analysis suggests that QFM is a powerful tool for studying spatial–temporal problems from the nanoscale to the megascale, as required in the design of the nanotube-based space elevator megacable.

3. Review on the mechanics of the space elevator cable

The equilibrium between gravitational and centrifugal forces for a portion of length dz ($z = 0$ fixed at the Earth's centre) of the space elevator cable implies (Pearson 1975)

$$\frac{dT}{dz} = -\rho A(z) g(z), \qquad g(z) = -\frac{GM}{z^2} + z\Omega^2 \qquad (3)$$

where T is the tension in the cable, A is its cross section area, G is the universal gravitational constant and M and Ω are respectively the mass and rotational speed of the Earth. Since $T = \sigma A$, with σ the stress in the cable, two main and complementary cases can be discussed: a constant cross section area A, for which $dT = A\,d\sigma$, or a uniform stress cable profile, for which $dT = \sigma\,dA$.

Integrating equation (3) assuming $A = $ constant yields

$$\frac{\sigma(z) - \sigma_0}{\rho} = GM\left(\frac{1}{z_0} - \frac{1}{z}\right) + \frac{1}{2}\Omega^2\left(z_0^2 - z^2\right). \qquad (4)$$

Note that the term on the rhs of equation (4) is only planet dependent. Assuming $\sigma_0 = 0$ at $z_0 = R^*$ (Earth's radius) and $\rho = 1300 \text{ kg m}^{-3}$ as for carbon nanotubes, the maximum stress is reached at GEO, i.e., at $z_{\text{GEO}} = (GM/\Omega^2)^{1/3} \approx 35\,800$ km where the gravitational and centrifugal forces are self-balanced. For the Earth $\sigma_{\max} = \sigma(z_{\text{GEO}}) \approx 63$ GPa ($R^* \approx 6.38 \times 10^6$ m, $M \approx 5.98 \times 10^{24}$ kg, $G \approx 6.67 \times 10^{-11} \text{ m}^3 \text{ kg}^{-1} \text{ s}^{-2}$). Incidentally, this value corresponds to the highest strength observed in the experiments by Yu *et al* (2000b) on multiwalled carbon nanotubes (MWCNT). Larger maximum stresses for more massive materials are expected to scale according to their density as described by equation (4). Thus, only today has the feasibility of the space elevator cable seemed to become realistic, as a consequence of the discovery of carbon nanotubes. By setting $T(z = R^* + L) = 0$ one derives the length L of the megacable to be globally under tension, as $L \approx 150\,000$ km (Pearson 1975). The cable length L can be reduced by a counterweight of mass m_c at z_c, quantifiable by satisfying the equilibrium of the mass, i.e., from $\sigma(z_c)A = g(z_c)m_c$. The cable volume is $V = AL$, to which the total mass will be proportional. The cable elastic extension can be evaluated as $\Delta L = \frac{1}{E} \int_R^{R^*+L} \sigma(z) \, \mathrm{d}z$.

Note that for a hypothetical compressive load, the slenderness ($s = L/\sqrt{I/A}$, with I the moment of inertia) corresponding to the transition between the tensional collapse and the Euler elastic instability is $s_C = \pi \sqrt{E/(\sigma_C(1 + a/L))}$, where E is the material Young modulus (e.g., 0.94 TPa for a [10, 10] carbon nanotube, according to the quantum mechanical calculations by Mielke *et al* (2004)), σ_C is its (compressive) strength and the first-order corrective term a/L has been derived assuming quantum elasticity. Thus, larger sensitivity to elastic instability is expected for smaller L/a and E/σ_C ratios (nanoscale). Yakobson *et al* (1996) studied the elastic instability of carbon nanotubes by using molecular dynamics. For a nanotube with length of 6 nm (and diameter of 1 nm) they found a critical strain of 0.09, whereas applying elasticity a critical value of 0.137 (Wang and Varadan 2005) would emerge. The discrepancy is explained by our correction if $a \approx 3.1$ nm ($0.137/0.09 = 1 + a/6$).

On the other hand, integrating equation (3) assuming $\sigma = \text{const}$ yields

$$\frac{A(z)}{A_0} = \exp\left\{\frac{\rho}{\sigma}\left[GM\left(\frac{1}{z} - \frac{1}{z_0}\right) + \frac{1}{2}\Omega^2\left(z^2 - z_0^2\right)\right]\right\} \tag{5}$$

that for $A = A_0$ at $z_0 = R^*$ gives a maximum area A_{GEO} at z_{GEO}, for which

$$\frac{A_{\text{GEO}}}{A_0} = \exp\left(0.776 R^* g_0 \frac{\rho}{\sigma}\right) \tag{6}$$

where $g_0 = g(z = R^*) \approx 9.78 \text{ m s}^{-2}$ is the gravity acceleration at the Earth's surface. The lhs term in equation (6) is the so-called taper ratio (Pearson 1975). For example, as anticipated, for steel this value is approximately 10^{33}, for Kevlar 2.6×10^8 and for carbon nanotubes 1.9: only today has the feasibility of the space elevator cable seemed to become realistic. The cable length L can be deduced satisfying the equilibrium of the counterweight, i.e., $\sigma A(z_c) = g(z_c)m_c$. The cable volume is $V = \int_R^{R^*+L} A(z) \, \mathrm{d}z$, approximately proportional to A_{GEO}/A_0. The cable elastic extension is $\Delta L = \frac{\sigma}{E}L$.

Now let us consider the dynamics of the cable. Since for carbon nanotubes the taper ratio is small, we can assume $\partial A/\partial z \approx 0$ in the motion equation of the cable, even if tapered. The effect of the taper ratio on the longitudinal vibrations of the cable was studied in detail by Pearson (1975). Here we are going to present just a simplification of the problem, according to Edwards (2003). The transverse or longitudinal vibrations of the cable can be deduced by solving the classical equation of the motion:

$$\frac{\partial^2 u}{\partial t^2} = \frac{Y}{\rho}\frac{\partial^2 u}{\partial z^2} \tag{7}$$

where u is the transverse or longitudinal displacement and $Y = \sigma$ for transverse and $Y = E$ for longitudinal oscillations. If the boundary conditions are both free or both fixed, the period of the oscillations is

$$P = \frac{2L}{q}\sqrt{\frac{\rho}{Y}} \tag{8}$$

where $q = 1, 2, 3, \ldots$ is an integer number. To avoid resonance P must be far from the period of the Moon (12.5 h), Sun (12 h) and Earth (24 h). Accordingly, considering the first mode $L \neq \frac{P}{2}\sqrt{\frac{Y}{\rho}}$, and for $\rho = 1300$ kg m^{-3}, $Y = \sigma = 63$ GPa, $L \neq 157\,000, 150\,000, 300\,000$ km. Resonance would imply transverse oscillations pumped by the Moon, Sun or Earth: thus, this problem has to be considered with caution, since we are close to the realistic cable length. However, the megacable length L can be modified by a counterweight, as previously described. It could also help in stabilizing the radial relative equilibrium of the megacable (Steindl and Troger 2005).

4. Atomic oxygen erosion/corrosion; micrometeorite and low Earth orbit object impacts

Damage nucleation in the cable is expected as distributed or localized, due to space debris erosion or impacts. In particular, atomic oxygen erosion will take place between 60 and 800 km, with the highest density around 100 km altitude (see Edwards 2000, 2003). The classical theory of erosion (see Carpinteri and Pugno 2004) assumes the material removal as proportional to the kinetic energy of the erosive particles, and consequently

$$\frac{1}{2}v_o^2\frac{dm_o}{dt} = k\frac{dV}{dt} \tag{9a}$$

where v_o is the velocity of the atomic oxygen mass flux dm_o/dt impacting on the cable volume V; the constant k denotes the erosion resistant of the cable material. Accordingly,

$$\frac{dH}{dt} = \frac{\rho_o v_o^3}{2k} = K \tag{9b}$$

where ρ_o is the atomic oxygen density and H is the cable thickness.

Analogously, micrometeorite impacts, arising between 500 and 1700 km with the highest density around 1000 km altitude (see Edwards 2000, 2003), will cause holes and/or craters in the cable. Particularly dangerous are the Leonid meteors, that traverse our solar system each 33 years, and that are expected in 2031. The Leonid debris includes dust particles and objects up to 10 cm in diameter, and some debris is always permanent.

The removed volume after an impact can be estimated using expressions similar to equations (9):

$$\tfrac{1}{2}v_m^2 m_m = k'\Delta V \tag{10a}$$

where v_m is the velocity of the micrometeorite with mass m_m, creating a crater of volume ΔV; the constant k' denotes the impact resistance of the cable material. Accordingly,

$$\frac{\Delta V}{V_m} = \frac{\rho_m v_m^2}{2k'} = K' \tag{10b}$$

where ρ_m is the meteorite density and V_m is its volume.

Roughly speaking, for large fragmentations $k \approx k' \approx \sigma_C$, where σ_C is the macroscopic material strength (Carpinteri and Pugno 2002); we can speculate that this estimate will remain valid at all size scales if the corresponding size-dependent value for the structural strength σ_C is considered (larger at the nanoscale, as a consequence of approaching the theoretical

strength σ_{th}). For atomic oxygen erosion, assuming plausible values of $\sigma_C \approx 10$ GPa, $\rho_o \approx 10^{-8}$ kg m^{-3} and $v_o \approx 1$ km s^{-1}, we deduce $K \approx 10^{-9}$ m s^{-1}, comparable with the experimental value of $K \approx 1$ mm/month $\approx 3 \times 10^{-9}$ m s^{-1} (see Edwards 2003). However, we have to note that here erosion is coupled with corrosion and thus that the process is more complex than as described. Similarly, for plausible values of $\sigma_C \approx 10$ GPa, $\rho_m \approx 3000$ kg m^{-3} and $v_m \approx 10$ km s^{-1} we deduce $K' \approx 15$, comparable with the value $K' \approx 50$ suggested by Edwards (2003). Thus, for nanofragmentation we could roughly estimate a material removal of $\Delta V \approx E_K/\sigma_{th}$ where E_K denotes the kinetic energy of the projectile.

Equations (9) predict a steady-state erosion, whereas a catastrophic failure was experimentally deduced by treating data recorded on the MIR space station by applying a fractal theory of erosion, in which the main assumption is the replacement of the volumes in equations (9a) and (10a) with their fractal counterparts (i.e., the fractal domain of the energy dissipation, between a Euclidean surface and volume; Carpinteri and Pugno 2002, 2004). Thus equations (9) and (10) are not conservative; however a coating layer (e.g., of gold, platinum or aluminium) is expected to improve the protection of the cable against erosion/corrosion and micrometeorite impacts (Edwards 2003).

According to equation (10b) objects larger than $\sim$10 cm could destroy the cable. Low Earth orbit objects (satellites and space debris larger than 10 cm) are tracked by US Space Command ($\sim$8000 objects). The probability of an impact of such an object on the cable is once over 250 days and could be avoided by controlling the cable position (Edwards 2003). However, in the case of cable cut the scenario could be the following. The elastic energy per unit volume cumulated in the cable is of the order of $\psi = (1/2)\sigma^2/E \approx (1/2)(63 \times 10^9)^2 10^{-12} \approx 2$ T J m^{-3}. Breaking the cable will result in a pair of de-tensioning waves moving apart at the speed of $c = \sqrt{E/\rho} \approx \sqrt{10^{12}/1300} \approx 28$ km s^{-1}. This would lead to a fragmentation of the cable, especially of the lower portion of it, as it returns to Earth and encounters our atmosphere. According to the design proposed by Edwards (2000, 2003) carbon nanotube bundles $\sim$1 cm long will work in parallel and will be connected in series by epoxy junctions; since the cable is expected to be 91 Mm long (a counterweight will be present) and the junction will be melted due to friction with the atmosphere, the total cable is expected to be fragmented into $\sim$10^{10} segments (a terrorist attack would yield the same scenario).

5. The strength of a real, thus defective, carbon nanotube-based space elevator megacable

In this section we present different deterministic and statistical models for predicting the strength of a real, thus defective, carbon nanotube-based space elevator cable. In addition to the previously discussed damage sources we expect unavoidable pre-existing defects in the cable simply for statistical reasons (Carpinteri and Pugno 2005), ultimately governed, but not controlled, by the production process. In fact, as we have not been able to build a large glass cable possessing the strength of a glass whisker, the principle of maximum likelihood ratio suggests to us that we will face a similar limit during the practical realization of the space elevator cable. In other words, a defect-free huge cable is statistically unrealistic. In spite of this, it is assumed in the current design (Edwards 2000, 2003). Accordingly, we have to take into account the presence of defects to treat a real cable.

Two different hypotheses of interaction between parallel nanotubes are plausible, depending on the cable construction: weak (i) or strong (ii) coupling. These two limits correspond to the two main practical realizations of the nanotube-based cable: (i) with parallel and independent nanotubes, (ii) in the case of forced interaction caused by transverse diagonal fibres; in both cases the nanotubes are connected to form a 'string' by epoxy junctions (see

Edwards 2003). The same behaviours could be obtained with a nanotube rope designed as a macroscopic rope, i.e., without (i) or with (ii) a twisting angle (with an optimal value for nanotube load transfer around 120°; see Qian *et al* 2003). In the former solution (i) 1 cm long nanotubes making up the ribbon will be parallel and overlap in the composite sections about 1 mm thick, whereas in the latter (ii) the cable will consist of both straight fibres under tension running the length of the cable and crossed diagonal fibres to take up and distribute the load in the case of meteor damage (a solution approximately 64% heavier than the first one; see Edwards 2003).

We are going to show that both these hypotheses and considering both deterministic (LEFM, Griffith 1921; QFM, Pugno 2002, 2004a, 2004b, 2006a, 2006b; Pugno and Ruoff 2004) and statistical approaches (Weibull 1939; nanoscale Weibull statistics, i.e., NWS, Pugno and Ruoff 2006; Pugno 2004a, 2006a) yield the same prediction: the strength of a real space elevator cable is expected to be reduced by a factor of at least ∼70% with respect to the theoretical carbon nanotube strength. Thus, it is the author's opinion that, as designed today, the cable will break.

Weak coupling (i). This seems to be the most promising solution, as proposed by Edwards (2003). In such a case even if a nanotube breaks, it produces almost no effect on the others, due to the weak coupling between them. A crack is blocked and the chain reaction of fracture is terminated (Yakobson and Smalley 1997). Unfortunately this positive behaviour has a negative counterpart, never mentioned in the extensive space elevator literature: just a single vacancy in a nanotube greatly affects its strength.

To demonstrate this we consider the atomistic simulations on strength of defective carbon nanotubes performed by Belytschko *et al* (2002), Mielke *et al* (2004) and Zhang *et al* (2005) and we compare their results with the related QFM predictions. Nanocracks of size n (number of adjacent atomic vacancies) or nanoholes of size m are considered: the index $m = 1$ corresponds to the removal of an entire hexagonal ring, $m = 2$ to the additional removal of the six hexagons around the former one (i.e., the adjacent perimeter of (18) atoms), $m = 3$ to the additional removal of the neighbouring 12 hexagonal rings (next adjacent perimeter), and so on. Quantum mechanics (QM) semiempirical calculations (PM3 method) and molecular mechanics (MM) calculations (with a modified Tersoff–Brenner potential of second generation (MTB-G2) or a modified Morse potential (M)) are reported and extensively compared with the QFM predictions in table 1. The comparison shows a relevant agreement, confirming and demonstrating that just a few vacancies can dramatically reduce the strength of a single nanotube. In particular, Belytschko *et al* (2002) performed atomistic molecular mechanics simulations on the fracture strength of a defective nanotube containing n adjacent atomic vacancies, as reported in table 1. The comparison with equation (11) is also depicted in figure 2 for the [80, 0] nanotube (QFM (continuous line) versus atomistic simulations (points)): in such a figure the two limit defects, a nanohole and a nanocrack, are compared for similar sizes n; note the asymptotic behaviour $\sigma_f \propto n^0$ for holes and $\sigma_f \propto n^{-1/2}$ for cracks, on increasing the defect size $n = 2R/a = 2l/a$.

After having demonstrated the validity of QFM by this extensive comparison, we treat the experimental results reported by Yu *et al* (2000a, 2000b) on single-walled carbon nanotube (SWCNT) ropes or on multiwalled carbon nanotubes (MWCNT) grown by arc discharge. Both the experiments were able to give a prediction of the fracture strength of a single-walled carbon nanotube, assuming for the nanotube rope/multiwalled nanotube the load carried only by the external nanotubes/shell. The ropes were supposed to be composed of [10, 10] nanotubes, thus with a diameter of 1.36 nm, arranged in the close-packed hexagonal structure, at a 'contact' distance of 0.34 nm. In table 2 the experimental measurements are reported and rationalized by applying QFM (i.e., by setting $\sqrt{\langle K^2 \rangle_a} = K_C$), assuming the presence of n adjacent atomic

Table 1. Atomistic simulations (Belytschko *et al* 2002, Mielke *et al* 2004, Zhang *et al* 2005) and QFM (Pugno and Ruoff 2004) predictions for a nanocrack of size *n* (number of adjacent atomic vacancy) or nanohole of size *m*. The index *m* = 1 corresponds to the removal of an entire hexagonal ring, *m* = 2 corresponds to the additional removal of the six hexagons around the former one (i.e., the adjacent perimeter of (18) atoms), *m* = 3 considers in addition the removal of the neighbouring 12 hexagonal rings (next adjacent perimeter), and so on. Quantum mechanics (QM) semiempirical calculations (PM3 method) and molecular mechanics (MM) calculations (modified Tersoff–Brenner potential of second generation (MTB-G2), or modified Morse potential (M)). The symbol (+H) means that the defect was saturated with hydrogen. Symmetric and asymmetric bond reconstructions were also considered (see Mielke *et al* 2004, Zhang *et al* 2005 for details). The tubes are 'short', if not otherwise specified: note that for long tubes a reduction in the strength is always observed, as an intrinsic size effect. For nested nanotubes an increment in the strength of ∼5 GPa is here assumed to roughly take into account the van der Waals (vdW) interaction between the walls.

Nanotube type	Nanocrack (*n*) and nanohole (*m*) sizes	Strength (GPa) by QM (MTB-G2) and MM (PM3; M) atomistic or QFM calculations
[5, 5]	Defect free	105 (MTB-G2); 135 (PM3)
[5, 5]	*n* = 1 (sym. +H)	85 (MTB-G2); 106 (PM3)
[5, 5]	*n* = 1 (asym. +H)	71 (MTB-G2); 99 (PM3)
[5, 5]	*n* = 1 (asym.)	70 (MTB-G2); 100 (PM3)
[5, 5]	*n* = 2 (sym.)	71 (MTB-G2); 105 (PM3)
[5, 5]	*n* = 2 (asym.)	73 (MTB-G2); 111 (PM3)
[5, 5]	*m* = 1 (+H)	70 (MTB-G2), 68 for long tube; 101 (PM3)
[5, 5]	*m* = 1–2 (+H)	50 (MTB-G2), 47 for long tube; 76 (MTB-G2)
[5, 5]	*m* = 2 (+H)	53 (MTB-G2), 50 for long tube; 78 (PM3)
[5, 5]	Stone–Wales	89 (MTB-G2), 88 for long tube; 125 (PM3)
[10, 10]	Defect free	88 (MTB-G2); 124 (PM3)
[10, 10]	*n* = 1 (sym. +H)	65 (MTB-G2)
[10, 10]	*n* = 1 (asym. +H)	68 (MTB-G2)
[10, 10]	*n* = 1 (sym.)	65 (MTB-G2); 101 (PM3)
[10, 10]	*n* = 2 (sym.)	64 (MTB-G2); 107 (PM3)
[10, 10]	*n* = 2 (asym.)	65 (MTB-G2); 92 (PM3)
[10, 10]	*m* = 1 (+H)	56 (MTB-G2), 52 for long tube; 89 (PM3)
[10, 10]	*m* = 1–2 (+H)	56 (MTB-G2), 46 for long tube; 84 (PM3)
[10, 10]	*m* = 2 (+H)	42 (MTB-G2), 36 for long tube; 67 (PM3)
[50, 0]	Defect free	89 (MTB-G2)
[50, 0]	*m* = 1 (+H)	58 (MTB-G2); 60 (QFM)
[50, 0]	*m* = 2 (+H)	46 (MTB-G2); 43 (QFM)
[50, 0]	*m* = 3 (+H)	40 (MTB-G2); 37 (QFM)
[50, 0]	*m* = 4 (+H)	36 (MTB-G2); 35 (QFM)
[50, 0]	*m* = 5 (+H)	33 (MTB-G2); 33 (QFM)
[50, 0]	*m* = 6 (+H)	31 (MTB-G2); 32 (QFM)
[100, 0]	Defect free	89 (MTB-G2)
[100, 0]	*m* = 1 (+H)	58 (MTB-G2); 60 (QFM)
[100, 0]	*m* = 2 (+H)	47 (MTB-G2); 43 (QFM)
[100, 0]	*m* = 3 (+H)	42 (MTB-G2); 37 (QFM)
[100, 0]	*m* = 4 (+H)	39 (MTB-G2); 35 (QFM)
[100, 0]	*m* = 5 (+H)	37 (MTB-G2); 33 (QFM)
[100, 0]	*m* = 6 (+H)	35 (MTB-G2); 32 (QFM)
[29, 29]	Defect free	101 (MTB-G2)
[29, 29]	*m* = 1 (+H)	77 (MTB-G2); 67 (QFM)
[29, 29]	*m* = 2 (+H)	62 (MTB-G2); 48 (QFM)
[29, 29]	*m* = 3 (+H)	54 (MTB-G2); 42 (QFM)
[29, 29]	*m* = 4 (+H)	48 (MTB-G2); 39 (QFM)
[29, 29]	*m* = 5 (+H)	45 (MTB-G2); 37 (QFM)

Table 1. (Continued.)

Nanotube type	Nanocrack (n) and nanoholes (m) sizes	Strength (GPa) by QM (MTB-G2) and MM (PM3; M) atomistic or QFM calculations
[29, 29]	$m = 6$ (+H)	42 (MTB-G2); 36 (QFM)
[47, 5]	Defect free	89 (MTB-G2)
[47, 5]	$m = 1$ (+H)	57 (MTB-G2); 61 (QFM)
[44, 10]	Defect free	89 (MTB-G2)
[44, 10]	$m = 1$ (+H)	58 (MTB-G2); 61 (QFM)
[40, 16]	Defect free	92 (MTB-G2)
[40, 16]	$m = 1$ (+H)	59 (MTB-G2); 63 (QFM)
[36, 21]	Defect free	96 (MTB-G2)
[36, 21]	$m = 1$ (+H)	63 (MTB-G2); 65 (QFM)
[33, 24]	Defect free	99 (MTB-G2)
[33, 24]	$m = 1$ (+H)	67 (MTB-G2); 67 (QFM)
[80, 0]	Defect free	93 (M)
[80, 0]	$n = 2$	64 (M); 64 (QFM)
[80, 0]	$n = 4$	50 (M); 50 (QFM)
[80, 0]	$n = 6$	42 (M); 42 (QFM)
[80, 0]	$n = 8$	37 (M); 37 (QFM)
[40, 0] (nested by a [32, 0])	Defect free	99 (M)
[40, 0] (nested by a [32, 0])	$n = 2$	73 (M); 73 (QFM + vdW interaction $\sim$5 GPa)
[40, 0] (nested by a [32, 0])	$n = 4$	57 (M); 58 (QFM + vdW interaction $\sim$5 GPa)
[40, 0] (nested by a [32, 0])	$n = 6$	50 (M); 50 (QFM + vdW interaction $\sim$5 GPa)
[40, 0] (nested by a [32, 0])	$n = 8$	44 (M); 44 (QFM + vdW interaction $\sim$5 GPa)
[100, 0]	$n = 4$	50 (M)
[40, 40]	$n = 4$	54 (M)

vacancies, i.e., a nanocrack of length $2l = na$:

$$\sigma_{\rm f} = K_C \sqrt{\frac{1 + \rho/2a}{\pi\,(l + a/2)}} = \sigma_{\rm th}\sqrt{\frac{1 + \rho/2a}{1 + 2l/a}}, \qquad \sigma_{\rm th} = \frac{K_{IC}}{\sqrt{\pi/2a}} \tag{11}$$

where $\rho \approx a/2$ is the crack tip radius (note that LEFM, i.e., $K = K_C$, would give the trivial prediction of equation (11) in the limit case of ρ/a, $a/l \rightarrow 0$). We have again assumed for consistency the fracture quantum a as coincident with the distance between two adjacent chemical bonds. Obviously, like equation (1), equation (11) assumes no interaction between defect and boundary. In table 2 we have assumed values of n for the highest measured strength in order to obtain plausible theoretical strength, which must be, as is well known, around 100 GPa; see table 1; the corresponding theoretical strength ($n = 0$) is thus quantified. We note that pinhole defects seem to be more realistic than adjacent atomic vacancies, not only for chemical reasons but also as a consequence of the space debris impacts, sources of nanoholes rather than of nanocracks. Assuming large holes ($R/a \rightarrow \infty$) and applying QFM, we predict $(\sigma_{\rm th} - \sigma_{\rm f})/\sigma_{\rm th} \rightarrow 70\%$. However note that in the experiments larger strength reductions were observed, suggesting the presence of more critical defects, such as elliptical holes or even truly nanocracks. Similarly, for the independent carbon nanotubes in the megacable the most plausible expectation is a strength reduction by a factor of at least $\sim$70%.

An additional data set on MWCNT tensile experiments is available today (Barber *et al* 2005); see table 3. However, the very large highest measured strength denotes an interaction between the external and internal walls, as pointed out by the same authors. Thus, the

Table 2. QFM (Pugno and Ruoff 2004) applied to SWCNT assuming the presence of nanocracks, i.e., *n* adjacent atomic vacancies: fracture strength extracted from single-walled carbon nanotube (SWCNT, Yu *et al* 2000a) ropes or multiwalled carbon nanotubes (MWCNT, Yu *et al* 2000b) nanotensile tests. Note that the case corresponding to the prediction of an ideal strength of 80.6 GPa (too small) is unlikely.

	Strength (GPa) SWCNT ropes (nanotensile tests)	Number n of atomic vacancies (QFM)			Strength (GPa) MWCNT (nanotensile tests)	Number n of atomic vacancies (QFM)	
1	13	79	63	47	11	97	130
2	15	59	47	35	12	82	109
3	16	52	41	31	18	36	48
4	17	46	36	27	18	36	48
5	22	27	21	16	19	32	43
6	23	25	19	14	20	29	39
7	25	21	16	12	20	29	39
8	29	15	12	9	21	26	35
9	32	12	10	7	24	20	27
10	33	11	9	6	24	20	27
11	37	9	7	5	26	17	22
12	43	6	5	3	28	14	19
13	45	6	4	3	34	9	13
14	48	5	4	3	35	9	12
15	**52**	**4**	**3**	**2**	37	8	11
16					37	8	11
17					39	7	9
18					43	5	8
19					**63**	**2**	**3**
Predicted ideal strength (GPa)		*104.0*	*93.0*	*80.6* *(unlikely)*		*97.6*	*112.7*

measured strength cannot be considered plausible for describing the strength of a SWCNT. Furthermore, in table 3 we have assumed $n = 0$ for the highest measured value of 259.7 GPa (ideal strength), or alternatively for the case of the measured value of 109.5 GPa (close to the plausible value of 100 GPa). Thus, in this last case and for the higher values of strengths, sites of interactions (here treated as 'negative' vacancies) between the two external layers have to be assumed; roughly speaking, the number of interaction sites can be estimated as the difference between the previous two cases, as described in table 3; and in the context of load transfer, sites of interactions are positive features. Note that we are just now going into the third-generation era of nanotensile tests (Zhu and Espinosa 2005), suggesting that in the future rigorous experiments, by simultaneous independent stress and strain monitoring, will be possible also at the nanoscale.

The tremendous defect sensitivity (i.e., large strength reduction due to small defects) discussed is confirmed by a statistical analysis based on NWS (Pugno and Ruoff 2006). According to this theory, the probability of failure F for a nearly defect-free nanotube under a tensile stress σ_f is independent of its volume (or surface), in contrast to classical Weibull statistics (1939), namely

$$F = 1 - \exp\left(\frac{\sigma_f}{\sigma_0}\right)^m. \tag{12}$$

The experimental data of Yu *et al* (2000a, 2000b) are treated with NWS in figures 3(a), (b). For the first data set $\sigma_0 \approx 33.9$ GPa (SWCNT), whereas for the second one (MWCNT) a

Table 3. QFM (Pugno and Ruoff 2004) applied to MWCNT: experiments on fracture strength extracted from MWCNT nanotensile tests (Barber *et al* 2005). Note the estimations of the interaction sites, treated as 'negative' vacancies (the difference between the columns 3 and 4 for lines 18–26 is always equal to 6, i.e., the number of vacancies that must be assumed in correspondence to a plausible ideal strength, starting from the wrong assumption of an ideal strength coincident with the highest measured value).

	Strength (GPa) (nanotensile tests)	Number n of atomic vacancies (QFM)	
1	17.4	277	49
2	22.3	169	29
3	23.7	149	26
4	30.0	93	16
5	44.2	42	7
6	49.3	34	5
7	52.7	29	4
8	54.8	27	4
9	62.1	21	3
10	66.2	18	2
11	84.9	11	1
12	90.1	9	1
13	90.3	9	1
14	91.1	9	1
15	99.5	8	1
16	101.6	7	0
17	108.5	6	0
18	**109.5**	6	**0**
19	119.1	5	*−1 (interaction)*
20	127.0	4	*−2 "*
21	132.9	4	*−2 "*
22	140.8	3	*−3 "*
23	141.0	3	*−3 "*
24	175.0	2	*−4 "*
25	231.8	1	*−5 "*
26	**259.7**	**0**	*−6 "*
Predicted ideal strength (GPa)		*(259.7)* *(unrealistic)*	*109.5*

comparable value $\sigma_0 \approx 31.2$ GPa is deduced, and for both data sets the nanoscale Weibull modulus is $m \approx 2.7$. The experiments by Barber *et al* (2005) are reported in figure 4, for which $\sigma_0 \approx 108.0$ GPa (but not significant for the strength of a single nanotube) and $m \approx 1.8$. Note that the 'nominal strength' σ_0 corresponds to a probability of failure of 63%; σ_0 is found statistically with respect to σ_{th}, reduced by a factor of about 70%, even if just a few vacancies are expected to be the cause of this tremendous reduction. Note that considering a partial transfer loading between the external and internal nanotubes/shells for SWCNT ropes/MWCNT would correspond to an additional 'geometrical' strength reduction. Furthermore, we have to emphasize that this definition of strength refers to a cross section annular area of a single atomic thick layer (0.34 nm) and thus the 'bulk' strength (referred to the compact circular area) is expected to be scaled down proportionally to the ratio between the effective and nominal cross section areas. However, for a single SWCNT and in this context (see equations (4) and (5)) this is just a matter of definition since the ratio σ/ρ is invariant.

Thus, also for the most promising solution (i), a strength reduction by a factor of at least 70% seems to be at the moment the most plausible expectation. This is due to the strong
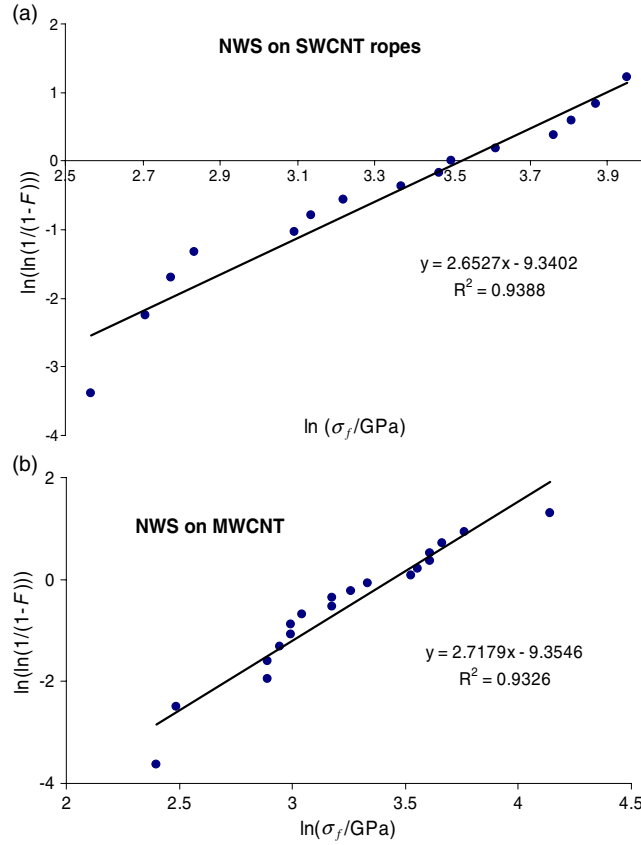
Figure 3. NWS (Pugno and Ruoff 2006) applied to SWCNT: experiments on fracture strength extracted from nanotensile tests on SWCNT ropes ((a); Yu *et al* 2000a) and on MWCNT ((b); Yu *et al* 2000b) grown by arc discharge.

strength reduction that just a few vacancies can produce (and their presence is statistically expected): roughly speaking, the effect of a single vacancy can be deduced from equation (1) considering $2R \approx a$, i.e., $x \approx 0.5$, for which $\sigma_f/\sigma_{th} \to 0.71$. The strength band $0.71\sigma_{th} - \sigma_{th}$ is thus forbidden, as a consequence of the crack quantization.

Strong coupling (ii). For such a case a single vacancy does not have this tremendous effect, as suggested by the fact that the fracture quantum will be of the order of the nanotube spacing, of the order of the nanotube diameter d, i.e., $a \approx d$, rather than—as in the previous case—of the order of the atomic size. Roughly speaking the effect of a vacancy can be deduced from equation (1) considering $2R \approx d/\lambda$, i.e., $x \approx 1/(2\lambda)$, where λ denotes the ratio between the nanotube diameter (the 'characteristic size' of the microstructure in the nanotube bundle) and the atomic size (the 'characteristic size' of the atomic structure in a single nanotube). We expect an even larger value for a than d at larger size scales, as a consequence of a larger cooperation between nanotubes. At any rate, the smallest plausible value for λ is ~ 10. Thus for $x \approx 1/20$, $\sigma_f/\sigma'_{th} \to 0.95$, where $\sigma'_{th} \approx \sigma_{th}/\sqrt{\lambda}$ denotes the new theoretical strength, assuming cooperation between nanotubes. And for $\sigma_{th} \approx 100$ GPa ($\lambda \approx 10$), $\sigma'_{th} \approx 32$ GPa whereas for $\lambda \approx 100$, $\sigma'_{th} \approx 10$ GPa: thus, a reduction by a factor of $\sim 70\%$ with respect to the theoretical carbon nanotube strength seems to be again unavoidable, even without defects.
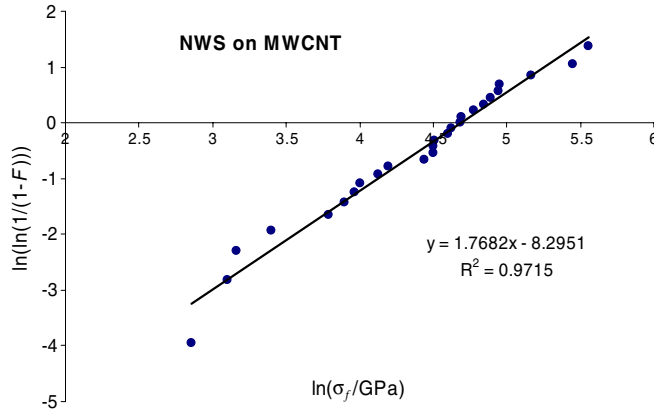
Figure 4. NWS applied to MWCNT: experiments on fracture strength extracted by nanotensile tests on MWCNT grown by chemical vapour deposition (Barber *et al* 2005).

A vacancy will additionally reduce the strength by a factor of about 5%, as previously deduced. Summarizing, for interacting nanotubes the presence of a defect is less critical but the ideal strength is intrinsically reduced, as synthetically described by

$$\frac{\sigma_{\rm f}}{\sigma_{\rm th}'} \approx \sqrt{\frac{1 + \rho/2d}{1 + 2l/d}}, \qquad \sigma_{\rm th}' \approx \frac{\sigma_{\rm th}}{\sqrt{\lambda}}. \tag{13}$$

Analogous to equation (11), equation (12) must be rewritten according to the coupling, namely as

$$F = 1 - \exp N_x^{\alpha} N_y^{\beta} N_z^{\gamma} \left(\frac{\sigma_{\rm f}}{\sigma_0}\right)^m \tag{14}$$

where N_x, N_y, and N_z are the number of nanotubes along x, y, z (longitudinal axis) respectively and α, β, γ are the corresponding scaling exponents. Weibull statistics (1939) basically assumes $\alpha = \beta = \gamma = 1$, with $N = N_x N_y N_z = V/V_0$, where V_0 is a characteristic volume, here assumed for consistency with equation (12) as the volume of a single nanotube (and V is the megacable volume). The constants σ_0 and m are in general different from those appearing in equation (12). According to equation (14), a size effect for the nominal strength is predicted:

$$\sigma_{\rm f} = \sigma_0 N_x^{-\alpha/m} N_y^{-\beta/m} N_z^{-\gamma/m}. \tag{15a}$$

The previous equation is simplified if one assumes Weibull statistics (1939):

$$\sigma_{\rm f} = \sigma_0 N^{-1/m}. \tag{15b}$$

For consistency with the previously treated case of $N = 1$, σ_0 in equations (12) and (14) or (15) must be the same. Equation (15b) is the simplest scaling law for a bundle composed of N nanotubes, each of them with (nominal) strength σ_0. The real problem is the determination of the three exponents in equation (15a) for the huge space elevator cable, or for simplicity the determination of m in equation (15b).

The experimental derivation of m is very complex. However, recently Zhang *et al* (2005) have been able to build the first metre-long cable based on carbon nanotubes. For such a nanostructured macroscopic cable a strength over density ratio of $\sigma/\rho \approx$ 120–144 kPa/(kg m^{-3}) was measured, dividing the breaking tensile force by the mass per unit length of the cable (the cross section geometry was not clearly identified). The cable density

was estimated to be $\rho \approx 1.5$ kg m^{-3}, thus resulting in a cable strength of $\sigma \approx 200$ kPa. Thus, we estimate for the single nanotube contained in such a cable $\sigma_f \approx 170$ MPa (carbon density of 1300 kg m^{-3}), exceptionally lower than its theoretical or measured nanoscale strength, as we expected according to the scaling of equations (15). For such a case, assuming the nanotubes investigated at the nanoscale to be 1 μm long and the cable 1 m in length, from equation (15b) we deduce $m \approx -\ln(1/10^{-6})/\ln(31/0.17) \approx 2.7$. We think that this value is only fortuitously coincident with that deduced by fitting the nanotensile experiments (that did not reveal size effects) with NWS; we expect a larger value as soon as the proposed experimental technique is improved for producing higher quality cables. Also, the power law in equations (15) is a too simplified; in fact applying equation (15b) with $m = 2.7$ will result in a vanishing megacable strength. Note that a densified cable with a larger value of $\sigma/\rho \approx 465$ kPa/(kg m^{-3}) was also realized, demonstrating the possibility of improving the technique (corresponding to $m \approx 3.3$). Now let us assume that we can apply the same equation (15b) to the results on force versus number of layers reported by Zhang *et al* (2005), just to have an idea about the scaling that we have to expect on varying the number of sheets in the megacable: since for 2 layers a breaking force of $\sim$40 mN was required, whereas for 12 layers a force of $\sim$235 mN was measured, and a linear dependence from the other tested cases of 4, 6, 8 and 10 layers was observed, we deduce $m \approx \ln(12)/\ln((12 \times 40)/(2 \times 235)) \approx 118$, thus larger than the previously computed value. Roughly, considering this value in the previous context, noting that the megacable volume is of the order of $10^8 \times 0.1 \times 10^{-6} = 10$ m^3 and a nanotube has a volume of the order of $10^{-8} \times 10^{-8} \times 10^{-6} = 10^{-22}$ m^3, a number of $N \approx 10^{23}$ nanotubes is expected, corresponding to a megacable strength of $\sigma_f \approx 34 \times (10^{23})^{-1/118} \approx 22$ GPa.

6. In-silicon experiments on the strength of the space elevator cable: the SE^3 code

The SE^3 code has, ad hoc, been developed for the in-silicon experiments of the space elevator cable and the related size effects, especially on strength. This code mainly gives as outputs the strength prediction and the damage space-time localization of the megarope. The stochastic inputs are the NWS describing the experimental strengths of the carbon nanoropes/tubes given by Yu *et al* (2000a, 2000b), i.e., $F \approx 1 - \exp(\frac{\sigma_f[\text{GPa}]}{34})^{2.7}$, and the nanotube Young's modulus $E \approx 0.94$ TPa deduced according to quantum mechanical simulations (density functional theory) by Mielke *et al* (2004).

Density functional theory simulations are based on the numerical solution of the Schrödinger's equation, and molecular mechanics or dynamics solve Newton's equation, deriving the generalized force from a given potential. Treating single particles or atoms with such methods is intrinsically limited in solving for objects at the atomic scale or nanoscale. In contrast, the SE^3 code is based on the global energy balance. The space elevator cable is assumed to be composed of weakly coupled (mean field solution) stochastic–linear elastic aligned SWCNTs (or ropes): basically a network of stochastic springs. Thus, the role played by a particle or an atom in the atomistic simulations is here played by an entire SWCNT (or rope), and thus the size limitation is correspondingly reduced. Imagine a virtual tensile experiment on a tapered space elevator cable: the uniform stress is increased in the cable, as in the tensile test of a cable with constant cross section area. Assuming a cable compliance C and stiffness $S = C^{-1}$, the total potential energy of the system is for T tension or δ displacement controls respectively ($T = S\delta$):

$$W = \tfrac{1}{2}S\delta^2 - T\delta = -\tfrac{1}{2}CT^2, \qquad \text{or} \qquad W = \tfrac{1}{2}S\delta^2. \tag{16}$$

The failure of the nanotube j ($1 < j < N$) will take place when the stress acting on it, σ_j, reaches the intrinsic nanotube strength σ_{fj}, stochastically distributed according to the failure

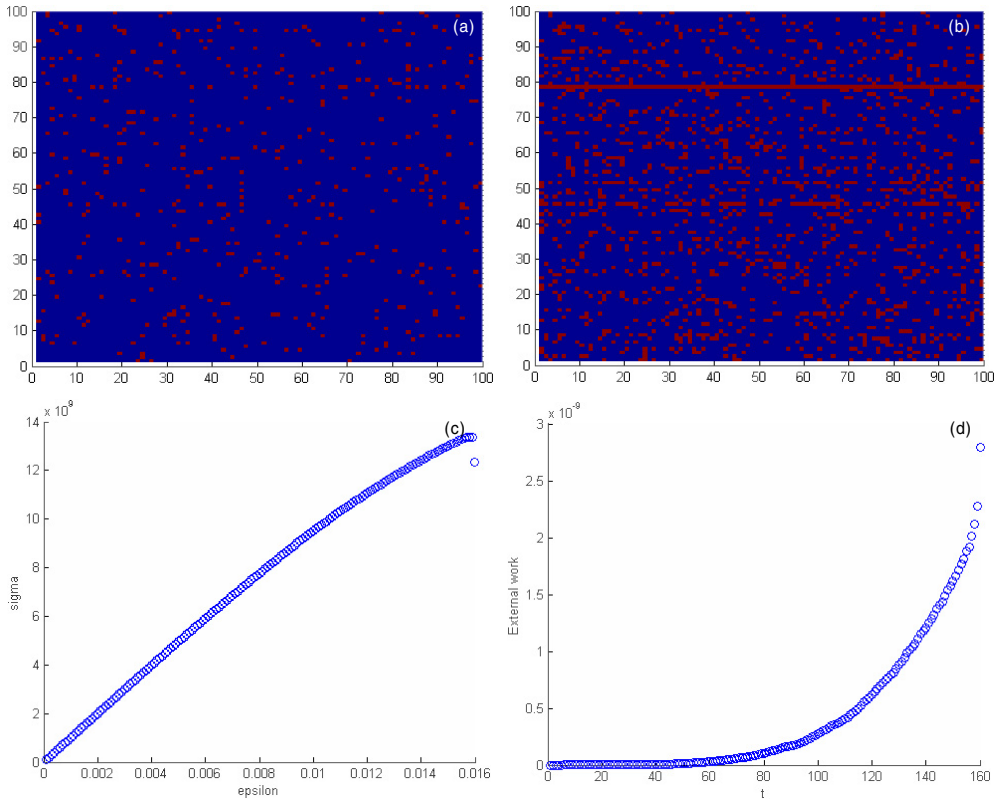**Figure 5.** 100×100 nanotube bundle. (a) Broken nanotubes after 1% of elongation. (b) Broken nanotubes at failure and damage localization. (c) Stress (GPa) versus strain for a nanotube bundle. (d) External work (N m) versus time (s). (e) Stored elastic energy (N m) versus time (s). (f) Dissipated energy (N m) versus time (s). (g) Kinetic energy (N m) emitted versus time (s). (h) Number of broken nanotubes versus time during the tensile test.

probability F (fitted to carbon nanotube nanotensile tests). The energy balance during failure implies

$$\Delta W_j + \Delta E_j + \Delta \Omega_j = 0 \tag{17}$$

where ΔE_j is the kinetic energy released and $\Delta \Omega_j$ is the dissipated energy (due to nanotube fracture); $\Delta \Omega_j = G_f \Delta A$ where G_f is the energy dissipated per unit area and ΔA is the nanotube cross section area; $\Delta W_j = -\frac{1}{2}T^2\Delta C$ and $\Delta W_j = \frac{1}{2}\delta^2\Delta S$ for tension and displacement controls respectively; ΔS and ΔC are the global variations imposed by the breakage of the nanotube j (trivial to evaluate—this is left to the reader). Accordingly, from the elastic energy $\Phi_j = \frac{1}{2}\frac{\sigma_{fj}^2}{E}\Delta A l^*$ stored in the nanotube (of length l^*) at fracture, the released kinetic, dissipated and stored energies, as well as the external work, can be easily computed. Space-time damage monitoring, stress–strain curves and related size effects can be accordingly deduced. An example of outputs for a two-dimensional simulation of a 100×100 network of nanotubes is reported in figure 5, assuming a displacement control linearly varying in time (t). Rather than a power law the numerical results suggest the validity of the size/shape scaling law
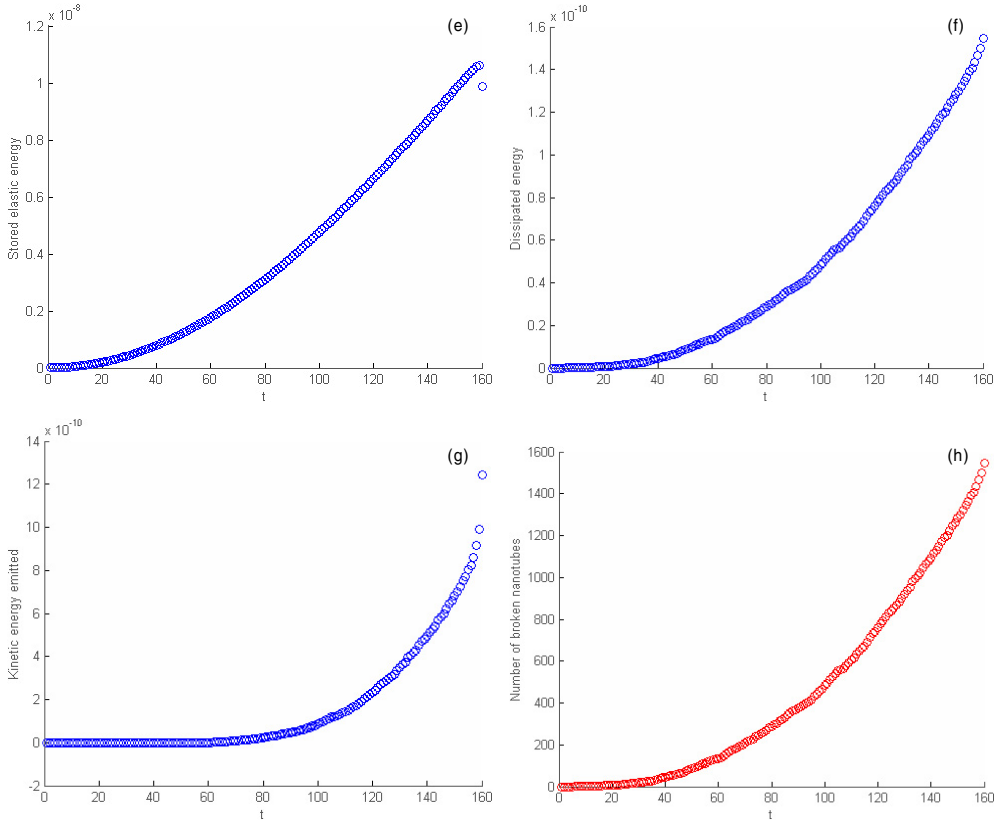
Figure 5. (Continued.)

proposed by Pugno (2006c):

$$\frac{\sigma_{\mathrm{f}}\,(S/V)}{\sigma_{\mathrm{nano}}} = \left(\frac{\left(\sigma_{\mathrm{nano}}/\sigma_{\mathrm{mega}}\right)^2 - 1}{\ell S/V + 1} + 1 \right)^{-1/2} \tag{18}$$

giving the failure strength σ_{f} for a structure of volume V and surface S with a nanostrength σ_{nano} and a megastrength σ_{mega}, where ℓ is a characteristic length. Note that such a scaling for the case of self-similar structures of size L ($L \propto \sqrt{S} \propto \sqrt[3]{V}$) having $\sigma_{\mathrm{nano}}/\sigma_{\mathrm{mega}} \to \infty$ agrees with the well-known Carpinteri scaling law (Carpinteri 1982). Preliminary results obtained by using the SE^3 code with $\sigma_{\mathrm{nano}} = \sigma_0 = 34$ GPa are fitted with $\sigma_{\mathrm{mega}} \approx 15$ GPa (and $\ell \ll L$). Thus again, the megarope is expected with a strength significantly reduced with respect to the ideal strength of a single nanotube.

7. Conclusions

Our results are based on both deterministic and statistical treatments, whether or not we consider interaction between the nanotubes in the megacable. For the last case (the current proposal) the maximum strength is predicted to be larger, but with extremely high defect sensitivity; in contrast, for the second case the situation is the opposite. In any case the strength of a real, thus defective, carbon nanotube-based space elevator megacable is expected

to be reduced by a factor of at least ∼70% with respect to the theoretical strength of a carbon nanotube, assumed in the current design. Such a reduction is sufficient to cast doubt on the effective realization of the space elevator. It is the author's opinion that the cable, if realized as designed today (see Edwards and Westling 2003), will break.

Acknowledgments

References

Artsutanov Y 1960 V Kosmos na Elektrovoze *Komsomol-skaya Pravda* (July) (contents described in Lvov 1967 *Science* **158** 946–947)

Barber A H, Kaplan-Ashiri I, Cohen S R, Tenne R and Wagner H D 2005 Stochastic strength of nanotubes: an appraisal of available data *Compos. Sci. Technol.* at press

Belytschko T, Xiao S P and Ruoff R 2002 Effects of defects on the strength of nanotubes: experimental–computational comparisons *Los Alamos National Laboratory preprint* physics/0205090

Brown E T and Hoek E 1978 Trends in relationship between measured *in situ* stresses and depth *Int. J. Rock Mech. Min. Sci. Geomech.* **15** 211–5

Carpinteri A 1982 Notch sensitivity in fracture testing of aggregative materials *Eng. Fract. Mech.* **16** 467–81

Carpinteri A and Pugno N 2002 A fractal comminution approach to evaluate the drilling energy dissipation *Int. J. Numer. Anal. Methods Geomech.* **26** 499–513

Carpinteri A and Pugno N 2004 Evolutionary fractal theory of erosion and experimental assessment on MIR space station *Wear* **257** 408–13

Carpinteri A and Pugno N 2005 Are the scaling laws on strength of solids related to mechanics or to geometry? *Nat. Mater.* **4** 421–3

Edwards B C 2000 Design and deployment of a space elevator *Acta Astronaut.* **10** 735–44

Edwards B C 2003 The Space Elevator NIAC Phases I and II Final reports

Edwards B C and Westling E A 2003 *The Space Elevator: A Revolutionary Earth-to-Space Transportation System* Spageo Inc.

Gombers J and Johnson P 2005 Dynamic triggering of earthquakes *Nature* **437** 830

Griffith A A 1921 The phenomenon of rupture and flow in solids *Phil. Trans. R. Soc.* A **221** 163–98

Iijima S 1991 Helical microtubules of graphitic carbon *Nature* **354** 56–8

Mielke *et al* 2004 The role of vacancy defects and holes in the fracture of carbon nanotubes *Chem. Phys. Lett.* **390** 413–20

Neuber H 1958 *Theory of Notch Stresses* (Berlin: Springer)

Novozhilov V 1969 On a necessary and sufficient criterion for brittle strength *Prikl. Mat. Mekh.* **33** 212–22

Pearson J 1975 The orbital tower: a spacecraft launcher using the Earth's rotational energy *Acta Astronaut.* **2** 785–99

Pugno N 2002 *A Quantized Griffith's criterion Italian Group of Fracture Mtg on Fracture Nanomechanics (Vigevano, Italy, Sept. 2002)*

Pugno N 2004a New quantized failure criteria: application to nanotubes and nanowires *Preprint* cond-mat/0411556

Pugno N 2004b *Preprint* cond-mat/0504520

Pugno N 2006a *Int. J. Fract.* at press

Pugno N 2006b Dynamic quantized fracture mechanics *Int. J. Fracture* at press

Pugno N 2006c A universal scaling law for nanoindentation, but not only *Preprint* cond-mat/0601370 (submitted)

Pugno N and Ruoff R 2004 Quantized fracture mechanics *Phil. Mag.* **84** 2829–45

Pugno N and Ruoff R 2006 Nanoscale Weibull statistics *J. Appl. Phys.* **99** 1–4 (*Preprint* cond-mat/0504518)

Qian D, Liu W K and Ruoff R S 2003 Load transfer mechanism in carbon nanotube ropes *Compos. Sci. Technol.* **63** 1561–9

Steindl A and Troger H 2005 Is the sky-hook configuration stable? *Nonlinear Dyn.* **40** 419–31

Wang Q and Varadan V K 2005 Stability analysis of carbon nanotubes via continuum models *Smart Mater. Struct.* **14** 281–6

Weibull W 1939 *A Statistical Theory of the Strength of Materials. Ingeniörsvetenskapsakademiens* Handlingar 151

Yakobson B I, Brabec C J and Bernholc J 1996 Nanomechanics of carbon tubes: instabilities beyond linear range *Phys. Rev. Lett.* **76** 2511–4

Yakobson B I and Smalley R E 1997 Fullerene nanotubes: C_1,000,000 and beyond *Am. Sci.* **85** 324–37

Yu M F, Files B S, Arepalli S and Ruoff R S 2000a Tensile loading of ropes of single wall carbon nanotubes and their mechanical properties *Phys. Rev. Lett.* **84** 5552–5

Yu M F, Lourie O, Dyer M J, Moloni K, Kelly T F and Ruoff R S 2000b Strength and breaking mechanism of multiwalled carbon nanotubes under tensile load *Science* **287** 637–40

Zhang M, Fang S, Zakhidov A A, Lee S B, Aliev A E, Williams C D, Atkinson K R and Baughman R H 2005 Strong, transparent, multifunctional, carbon nanotube sheets *Science* **309** 1215–9

Zhang S, Mielke S L, Khare R, Troya D, Ruoff R S, Schatz G C and Belytschko T 2005 Mechanics of defects in carbon nanotubes: atomistic and multiscale simulations *Phys. Rev.* B **71** 115403

Zhu Y and Espinosa H D 2005 An electromechanical material testing system for in situ electron microscopy and applications *Proc. Natl Acad. Sci. USA* **102** 14503–8